Stem Cell Reports, Volume *13*

Supplemental Information

ALDH-Dependent Glycolytic Activation Mediates Stemness and Paclitaxel Resistance in Patient-Derived Spheroid Models of Uterine Endometrial Cancer

Yutaro Mori, Kaoru Yamawaki, Tatsuya Ishiguro, Kosuke Yoshihara, Haruka Ueda, Ai Sato, Hirokazu Ohata, Yohko Yoshida, Tohru Minamino, Koji Okamoto, and Takayuki Enomoto

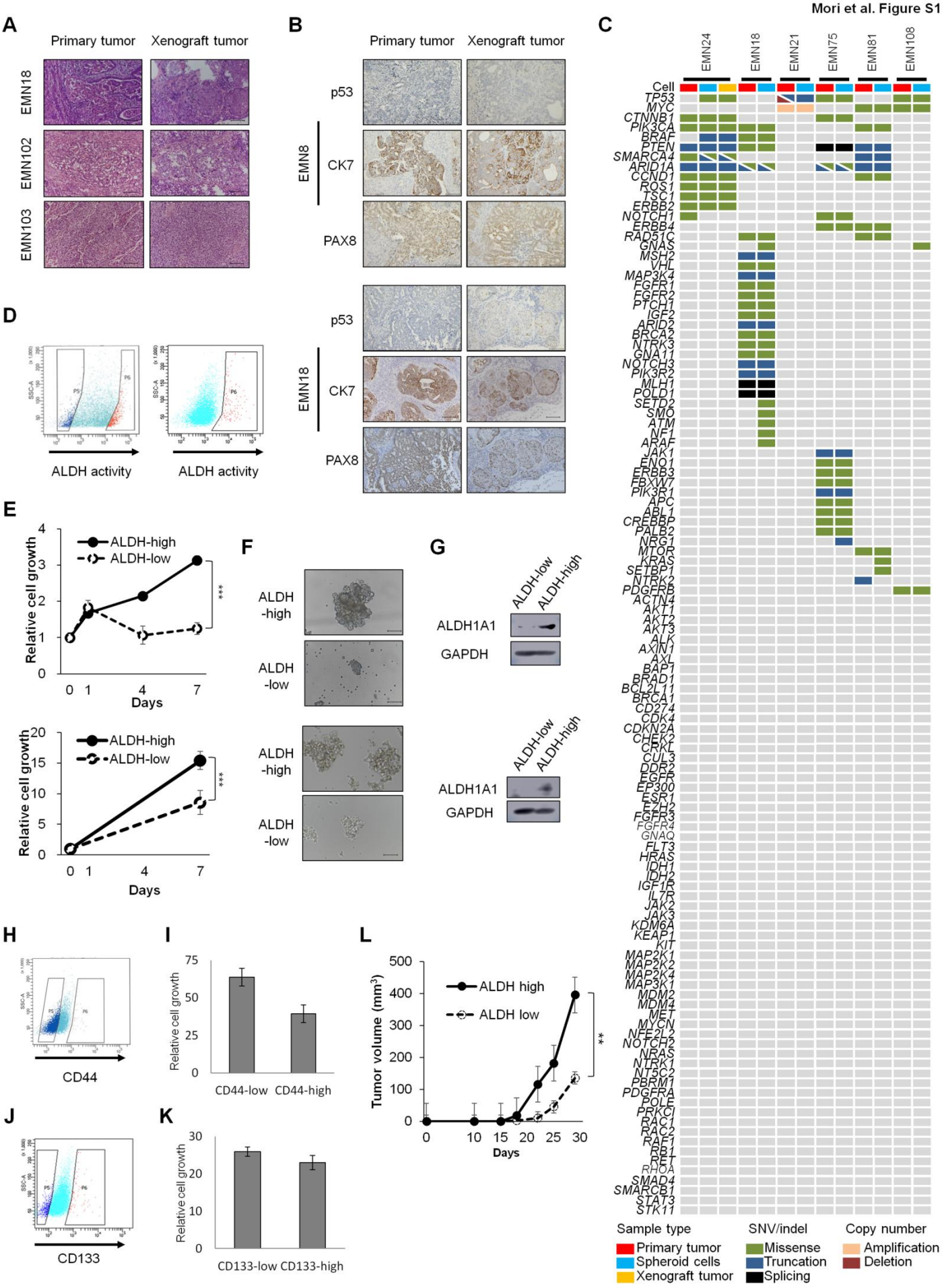
A
Primary tumor
Xenograft tumor
EMN18
EMN102
EMN103
B
Primary tumor
Xenograft tumor
p53
EMN8
CK7
PAX8
p53
EMN18
CK7
PAX8
C
EMN24
EMN18
EMN21
EMN75
EMN81
EMN108
Cell
TP53
MYC
CTNNB1
PIK3CA
BRAF
PTEN
SMARCA4
ARID1A
CCND1
ROS1
TSC1
ERBB2
NOTCH1
ERBB4
RAD51C
GNAS
MSH2
VHL
MAP3K4
FGFR1
FGFR2
PTCH1
IGF2
ARID2
BRCA2
NTRK3
GNA11
NOTCH3
PIK3R2
MLH1
POLD1
SETD2
SMO
ATM
NF1
ARAF
JAK1
ENO1
ERBB3
FBXW7
PIK3R1
APC
ABL1
CREBBP
PALB2
NRG1
MTOR
KRAS
SETBP1
NTRK2
PDGFRB
ACTN4
AKT1
AKT2
AKT3
ALK
AXIN1
AXL
BAP1
BRAD1
BCL2L11
BRCA1
CD274
CDK4
CDKN2A
CHEK2
CRKL
CUL3
DDR2
EGFR
EP300
ESR1
EZH2
FGFR3
FGFR4
GNAQ
FLT3
HRAS
IDH1
IDH2
IGF1R
IL7R
JAK2
JAK3
KDM6A
KEAP1
KIT
MAP2K1
MAP2K2
MAP2K4
MAP3K1
MDM2
MDM4
MET
MYCN
NFE2L2
NOTCH2
NRAS
NTRK1
NT5C2
PBRM1
PDGFRA
POLE
PRKCI
RAC1
RAC2
RAF1
RB1
RET
RHOA
SMAD4
SMARCB1
STAT3
STK11
Sample type
Primary tumor
Spheroid cells
Xenograft tumor
SNV/indel
Missense
Truncation
Splicing
Copy number
Amplification
Deletion
D
ALDH activity
ALDH activity
E
ALDH-high
ALDH-low
Relative cell growth
Days
***
ALDH-high
ALDH-low
Relative cell growth
Days
***
F
ALDH -high
ALDH -low
ALDH -high
ALDH -low
G
ALDH-low
ALDH-high
ALDH1A1
GAPDH
ALDH-low
ALDH-high
ALDH1A1
GAPDH
H
CD44
I
Relative cell growth
CD44-low
CD44-high
J
CD133
K
Relative cell growth
CD133-low
CD133-high
L
ALDH high
ALDH low
Tumor volume (mm3)
Days
**

Figure S1. Spheroid cells derived from human endometrial cancer showing the characteristics of CSCs with high ALDH activity. Related to Figure 1.

A, H&E staining of xenograft and primary tumors (EMN18, EMN102, and EMN103 cells). Scale bar, 100 μm. B, Immunostaining of xenograft and primary tumors with the indicated antibodies (EMN8 and EMN18 cells). Scale bar, 100 μm. C, Target sequencing analyses of primary tumor and spheroid cells. D, FACS analyses of ALDH activity after ALDEFLUOR staining (Left: EMN 8, Right: EMN21). Left gated population, ALDH-low cells; right gated population, ALDH-high cells (EMN8 cells). E, time course analyses of cell growth (Upper: EMN8, Lower: EMN21). n = 4 independent experiments, $p < 0.001$, Student's t-tests. F, Bright-phase images of spheroid formation after 7 days of *in vitro* cultivation (Upper: EMN8, Lower: EMN21). Scale bars, 100 μm. G, Western blot analyses of ALDH-high and ALDH-low cells after sorting (Upper: EMN8, Lower: EMN21). H, FACS analyses of CD44 expression (EMN24 cells). Left gated population, CD44-low cells; right gated population, CD44-high cells. I, Relative number of spheroid cells after *in vitro* cultivation for 7 days after sorting based on CD44 expression (EMN24 cells). n = 4 independent experiments, Student's t-tests. J, FACS analyses of CD133 expression (EMN24 cells). Left gated population, CD133-low cells; right gated population, CD133-high cells. K, Relative number of spheroid cells after *in vitro* cultivation for 7 days after sorting based on CD133 expression (EMN24 cells). n = 4 independent experiments, Student's t-tests. L, Volume (mean ± SEM) of xenograft tumors from 1×10^6 ALDH-low and ALDH-high cells (EMN21). n = 5 independent experiments, $p = 0.002$, Student's t-tests. **, $p < 0.01$; ***, $p < 0.001$.

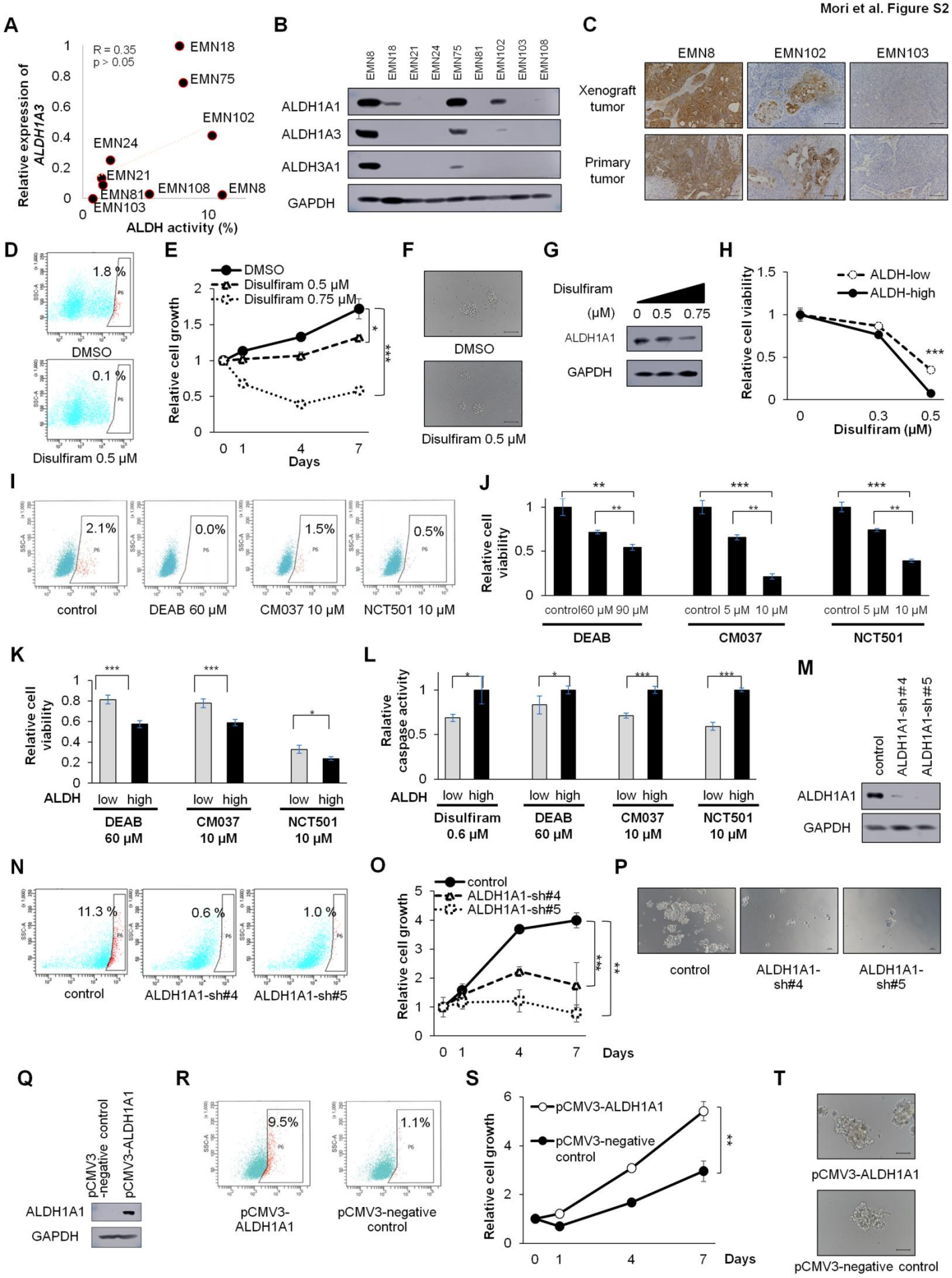
A
R = 0.35
p > 0.05
EMN18
EMN75
EMN102
EMN24
EMN21
EMN81
EMN108
EMN8
EMN103
Relative expression of ALDH1A3
ALDH activity (%)
B
EMN8
EMN18
EMN21
EMN24
EMN75
EMN81
EMN102
EMN103
EMN108
ALDH1A1
ALDH1A3
ALDH3A1
GAPDH
C
EMN8
EMN102
EMN103
Xenograft tumor
Primary tumor
D
1.8 %
DMSO
0.1 %
Disulfiram 0.5 μM
E
DMSO
Disulfiram 0.5 μM
Disulfiram 0.75 μM
Relative cell growth
Days
F
DMSO
Disulfiram 0.5 μM
G
Disulfiram (μM)
0 0.5 0.75
ALDH1A1
GAPDH
H
ALDH-low
ALDH-high
Relative cell viability
Disulfiram (μM)
I
2.1%
0.0%
1.5%
0.5%
control
DEAB 60 μM
CM037 10 μM
NCT501 10 μM
J
Relative cell viability
control 60 μM 90 μM
control 5 μM 10 μM
control 5 μM 10 μM
DEAB
CM037
NCT501
K
Relative cell viability
ALDH
low high
DEAB 60 μM
CM037 10 μM
NCT501 10 μM
L
Ralative caspase activity
ALDH
low high
Disulfiram 0.6 μM
DEAB 60 μM
CM037 10 μM
NCT501 10 μM
M
control
ALDH1A1-sh#4
ALDH1A1-sh#5
ALDH1A1
GAPDH
N
11.3 %
0.6 %
1.0 %
control
ALDH1A1-sh#4
ALDH1A1-sh#5
O
control
ALDH1A1-sh#4
ALDH1A1-sh#5
Relative cell growth
Days
P
control
ALDH1A1-sh#4
ALDH1A1-sh#5
Q
pCMV3-negative control
pCMV3-ALDH1A1
ALDH1A1
GAPDH
R
9.5%
1.1%
pCMV3-ALDH1A1
pCMV3-negative control
S
pCMV3-ALDH1A1
pCMV3-negative control
Relative cell growth
Days
T
pCMV3-ALDH1A1
pCMV3-negative control

Figure S2. Modification of ALDH affects the propagation and proliferation of spheroid cells. Related to Figure 2 and 3. A, Correlation between ALDH activity and *ALDH1A3* mRNA levels on culture day 10. B, Western blot analyses of spheroid cells on culture day 10. C, Immunostaining of ALDH1A1 in the indicated xenograft tumors and corresponding primary tumors. Scale bars, 100 μm. D, ALDH activity after treatment with DMSO or 0.5 μM disulfiram for 24 h (EMN81 cells). E, Time course of cell growth of the spheroids (EMN81 cells). n = 4 independent experiments, $p < 0.001$, Student's t-test. F, Bright-phase images of spheroids after disulfiram treatment for 7 days (EMN81 cells). Scale bars, 100 μm. G, Western blot analyses of spheroids after treatment with the indicated amounts of disulfiram for 24 h (EMN81 cells). H, Responses of ALDH-high and ALDH-low cells to different concentrations of disulfiram after incubation for 7 days (EMN81 cells). n = 4 independent experiments, $p < 0.001$, Student's t-test. I, ALDH activity after treatment with DMSO, 60 μM DEAB, 10 μM CM037, or 10 μM NCT501 for 24 h (EMN24 cells). J, Relative cell viability of spheroid cells after culture for 7 days with the indicated concentrations of ALDH inhibitor (EMN24 cells). n = 4 independent experiments, $p < 0.001$, Student's t-tests. K, Relative cell viability of ALDH-high and ALDH-low cells to ALDH inhibitor after incubation for 7 days (EMN24 cells). n = 4 independent experiments, Student's t-test. L, Relative caspase activity of ALDH-high and ALDH-low cells to ALDH inhibitor after incubation for 7 days (EMN24 cells). Student's t-tests. n = 4 independent experiments, Student's t-test. M, Western blot analyses after infection with the indicated lentiviruses (EMN8 cells). N, ALDH activity after ALDEFLUOR staining (EMN8 cells). O, Time course of proliferation of infected cells (EMN8 cells). n = 4 independent experiments, $p < 0.001$, Student's t-test. P, Bright-phase images of infected cells (EMN8 cells). Scale bars, 100 μm. Q, Western blot analyses of the spheroids after infection with the indicated lentiviruses (EMN21 cells). R, ALDH activity of the infected cells after ALDEFLUOR staining (EMN21 cells). S, Time course of proliferation of infected cells (EMN21 cells). n = 4 independent experiments, $p < 0.01$, Student's t-tests. T, Bright-phase images of the infected cells (EMN21 cells). Scale bars, 100 μm. *, $p < 0.05$; **, $p < 0.01$; ***, $p < 0.001$.

A

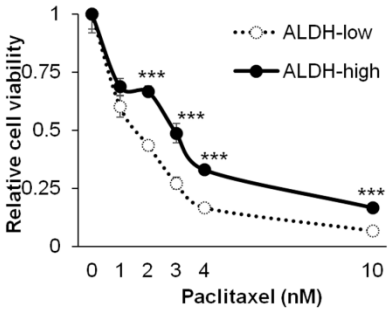

B

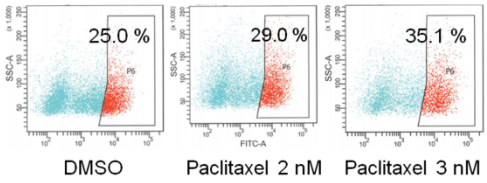

C

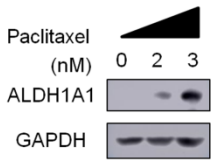

D

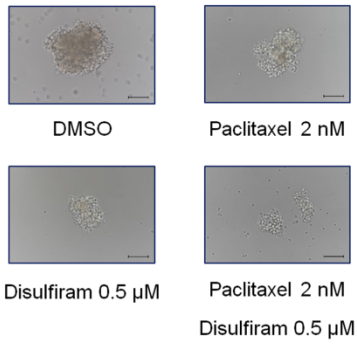

E

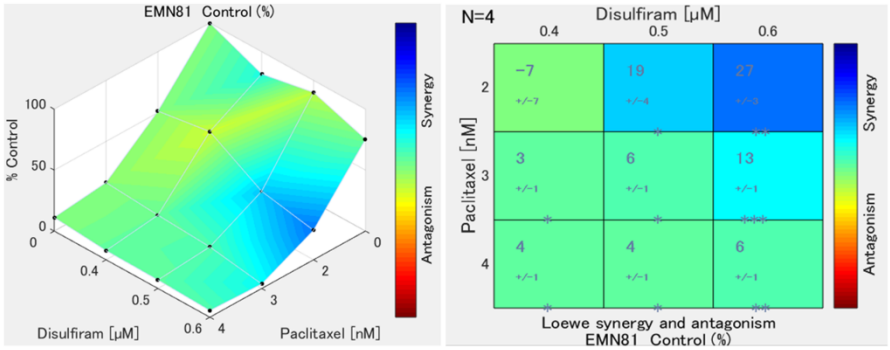

F

	Cell number							1/(stem cell frequency) (confidence intervals)
	64	32	16	8	4	2	1	
DMSO	6/12	3/12	2/12	1/12	1/12	1/12	0/24	89.6 (52.8-152)
Disulfiram	3/12	1/12	1/12	0/12	0/12	0/12	0/24	282.9 (118.5-677)
Paclitaxel	4/12	3/12	2/12	0/12	1/12	0/12	0/24	133.5 (71.6-249)
Paclitaxel Disulfiram	2/12	1/12	1/12	0/12	0/12	0/12	0/24	362 (136.2-963)

* * *

G

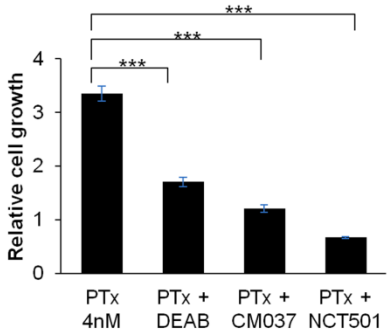

Figure S3. ALDH activity and expression are related to paclitaxel sensitivity of spheroid cells (EMN81 cells). Related to Figure 4. A, Responses of ALDH-high and ALDH-low cells to different concentrations of paclitaxel after incubation for 7 days. n = 4 independent experiments, $p < 0.001$, Student's t-tests. B, FACS analyses of ALDH activity in ALDH-high cells in the presence or absence of paclitaxel (7 days after the treatment). C, Western blot analyses of ALDH-high cells treated with paclitaxel for 7 days. D, Bright-phase images of spheroids after treatment with paclitaxel and disulfiram for 7 days. Scale bars, 100 μm. E, Relative cell viability of spheroid cells after culture for 7 days with the indicated concentrations of ALDH inhibitor and paclitaxel. Synergistic interaction was assessed with Combenefit software. n = 4 independent experiments. F, *in vitro* limiting dilution analysis for 14 days cultivation using spheroid cells exposed to disulfiram and/or paclitaxel *in vitro* for 7 days. G, Relative number of spheroid cells at 7 days after cultivation with paclitaxel and indicated ALDH inhibitor (EMN24 cells). n = 4 independent experiments, $p < 0.001$, Student's t-tests. *, $p < 0.05$; ***, $p < 0.001$.

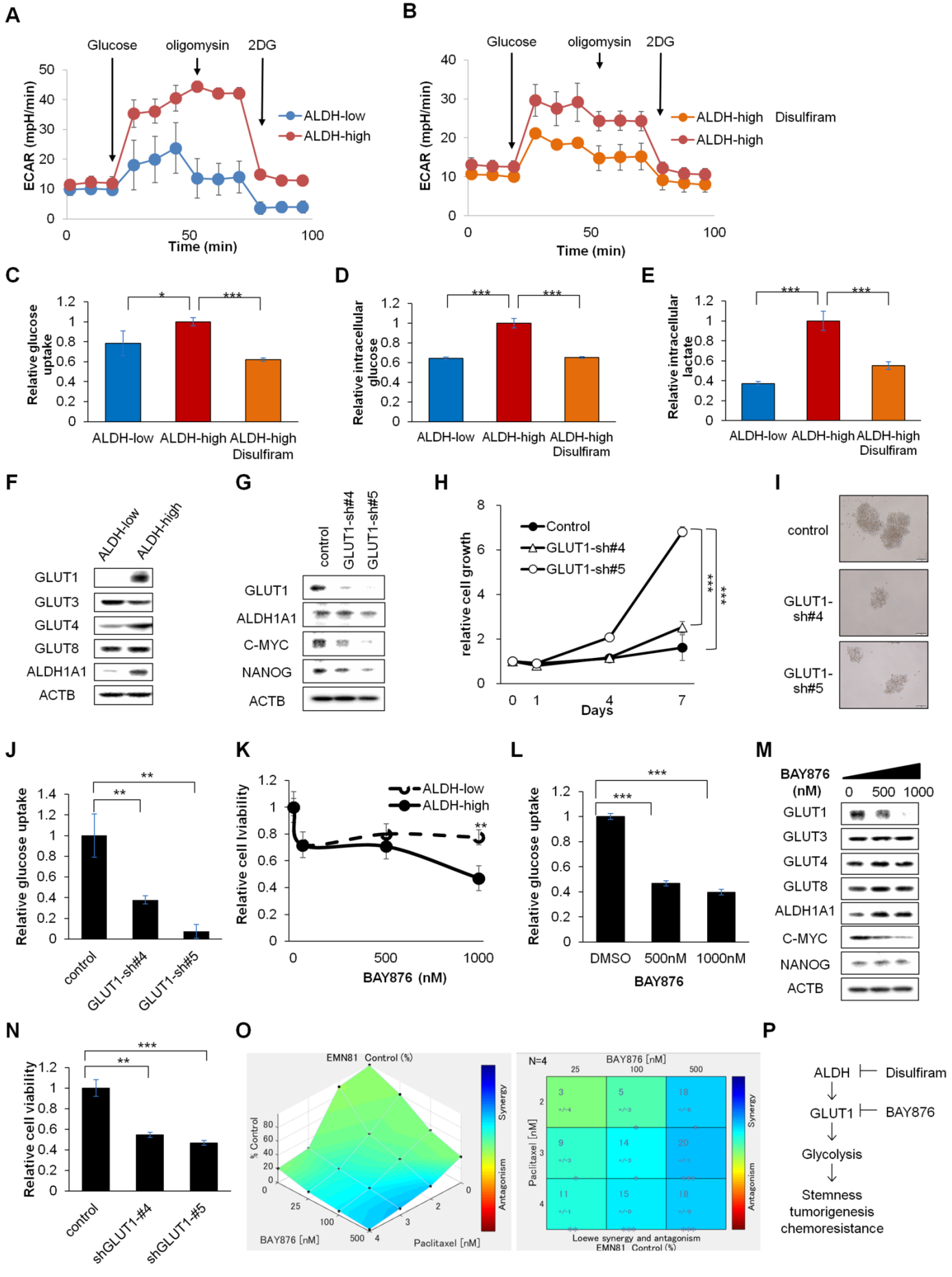
A
Glucose
oligomysin
2DG
ECAR (mpH/min)
Time (min)
ALDH-low
ALDH-high
B
Glucose
oligomysin
2DG
ECAR (mpH/min)
Time (min)
ALDH-high Disulfiram
ALDH-high
C
Relative glucose uptake
ALDH-low
ALDH-high
ALDH-high Disulfiram
D
Relative intracellular glucose
ALDH-low
ALDH-high
ALDH-high Disulfiram
E
Relative intracellular lactate
ALDH-low
ALDH-high
ALDH-high Disulfiram
F
ALDH-low
ALDH-high
GLUT1
GLUT3
GLUT4
GLUT8
ALDH1A1
ACTB
G
control
GLUT1-sh#4
GLUT1-sh#5
GLUT1
ALDH1A1
C-MYC
NANOG
ACTB
H
Control
GLUT1-sh#4
GLUT1-sh#5
relative cell growth
Days
I
control
GLUT1-sh#4
GLUT1-sh#5
J
Relative glucose uptake
control
GLUT1-sh#4
GLUT1-sh#5
K
ALDH-low
ALDH-high
Relative cell lviability
BAY876 (nM)
L
Relative glucose uptake
DMSO
500nM
1000nM
BAY876
M
BAY876 (nM)
0
500
1000
GLUT1
GLUT3
GLUT4
GLUT8
ALDH1A1
C-MYC
NANOG
ACTB
N
Relative cell viability
control
shGLUT1-#4
shGLUT1-#5
O
EMN81 Control (%)
% Control
BAY876 [nM]
Paclitaxel [nM]
Synergy
Antagonism
N=4
BAY876 [nM]
Paclitaxel [nM]
Loewe synergy and antagonism
EMN81 Control (%)
P
ALDH
Disulfiram
GLUT1
BAY876
Glycolysis
Stemness
tumorigenesis
chemoresistance

Figure S4. Combination therapy with paclitaxel and the GLUT1 inhibitor synergistically inhibits endometrial cancer cell progression (EMN81 cells). Related to Figure 6 and 7.

A-B, Time course of ECAR of spheroid cells with the indicated stimulation. The differences between ALDH-high and ALDH-low cells (A), and between ALDH-high cells with vehicle or disulfiram treatment (B). n = 4 independent experiments. C-E, Relative glucose uptake (C), intracellular glucose (D), and lactate level (E) of ALDH-low cells, ALDH-high cells, and ALDH-high cells treated with disulfiram. n = 4 independent experiments, $p < 0.01$, Student's t-test. F-G, Western blot analyses of ALDH-high and ALDH-low cells (F), and after infection with the indicated lentiviruses (G). H, Time course of the proliferation of the infected cells. n = 4 independent experiments, $p < 0.01$, Student's t-test. I, Bright-phase images of the infected cells. Scale bars, 100 μm. J, Relative glucose uptake of spheroid cells of the infected cells. n = 4 independent experiments, $p < 0.01$, Student's t-test. K-L, Relative cell viability (K) and glucose uptake (L) of spheroid cells after culture for 7 days with the indicated concentration of BAY876. n = 4 independent experiments, $p < 0.01$, Student's t-test. M, Western blot analyses of cells after exposure to the indicated concentration of BAY876. N, Relative cell viability of spheroid cells after culture for 7 days with 2 nM paclitaxel. n = 4 independent experiments, Student's t-test. O, Relative cell viability of spheroid cells with the indicated concentrations of BAY876 and paclitaxel *in vitro*. Synergistic interaction was assessed with Combenefit software. n = 4 independent experiments. P, A model of regulation of endometrial cancer stemness by ALDH and glycolysis. *, $p < 0.05$; **, $p < 0.01$; ***, $p < 0.001$.

Supplementary Table Legends

Table S1. Clinical data on endometrial cancer from which spheroid cells were obtained. Clinical stage was assigned according to the International Federation of Gynecology and Obstetrics (FIGO) staging system.

Table S2. Gene list of NCC oncopanel v4. Related to Figure 1 and Figure S1.

Table S3. The association between ALDH1A1 expression status and clinicopathological factors for 223 patients with early-stage and 35 patients with advanced-stage endometrial endometrioid cancer. Related to Figure 6.

Table S4. Association of ALDH1A1 expression with overall survival and progression-free survival in univariate analyses (35 cases of advanced disease). Related to Figure 6.

Table S5. Association of ALDH1A1 expression with overall survival and progression-free survival in multivariate analyses (35 cases of advanced disease). Related to Figure 6.

Table S6. List of antibodies used in this study

Supplemental Experimental Procedures

Tumor-derived spheroid culture

Endometrial cancer tissues were obtained from patients with primary endometrial cancer within 30 min of surgical excision. Tumor samples were placed on ice in phosphate-buffered saline (PBS) and transported to the laboratory. The samples were washed with PBS and mechanically cut into small pieces using a scalpel, followed by dissociation with 150 U/mL collagenase plus 50 U/mL hyaluronidase (Stemcell Technologies, Vancouver, BC, Canada) for 2 h at 37 °C. Dissociated cells were sequentially filtered through 100- and 70-μm cell strainers (BD Falcon). Collected cells were isolated through density gradient centrifugal purification in PBS containing Histodenz (Sigma, MO, USA). After lysis of red blood cells with ACK Lysing Buffer (Gibco), the remaining cells were grown on ultra-low-attachment culture dishes (Corning, NY, USA) in STEMPRO hESC SFM (Gibco) supplemented with 8 ng/mL basic fibroblast growth factor (Invitrogen, Carlsbad, CA, USA) and penicillin/streptomycin (37 °C, 5% CO_2). All dissociated cells from clinical samples formed sphere-like structures within 1 week. These spheroid cells grew stably *in vitro* after 1–6 months from the initial culture and continued to expand for more than 1 year. For serial passaging, spheroid cells were dissociated with Accumax (Innovative Cell Technologies) once every 14 days. For *in vitro* differentiation experiment, cells were cultivated with 10% FBS on standard attachment culture condition for 7 days.

Animal experiments

For drug efficacy studies, the mice were randomized into different groups. Disulfiram (40 mg/kg/day) and BAY876 (3.0 mg/kg/day) was administered five times/week, and paclitaxel (10 mg/kg/day) was administered three times/week, after injection of 1×10^5 spheroid cells. Mice were monitored every 3–4 days until 3–5 weeks after cell transplantation.

Targeted sequencing analysis

Genomic DNA samples were extracted from patient-derived frozen tumor tissues and spheroid cells. For targeted sequencing analysis, a SureSelect NCC Oncopanel v4 (Agilent Technologies) capturing all coding exons of 114 genes and translocated introns of 12 genes was used (Table S3). Sequencing libraries were constructed with a SureSelectXT Reagents Kit (Agilent Technologies) (Asano et al., 2017). Paired-end sequencing (2 x 150 bp) was performed on NextSeq 500 (Illumina, San Diego, CA, USA). Mutations (single-nucleotide variations and short insertions and deletions), gene amplifications, and gene fusions were detected using the cisCall (Clinical Sequence Call) system (Kato et al., 2018).

Gene set enrichment analysis (GSEA)

Microarray analyses were performed using Agilent Whole Human Genome 8 × 60 K oligo microarrays. Microarray data were accessible through the Gene Expression Omnibus database (accession number: GSE123530). Gene set enrichment analysis was performed using gene set collection version 6.2 from the Molecular Signatures Database (Subramanian et al., 2005, Mootha et al., 2003).

Flow cytometry analyses

Dissociated single spheroid cells were filtered, incubated with 7-AAD (BD Pharmingen) for exclusion of nonviable cells, and used for ALDEFLUOR assays (Stem Cell Technologies) or staining with antibody conjugated with phycoerythrin (Table S4). Xenograft tumors were enzymatically dissociated, and cancer cells were purified using a Mouse Cell Depletion Kit (Miltenyi Biotec). Samples were analyzed and sorted using a FACS Aria II Cell Sorter (BD Biosciences).

Cell-based assay

Cell viability was quantified by using CellTiter-Glo Luminescent Cell Viability Assays (Promega, Madison, WI, USA), and caspase-3/7 activity was quantified by using Caspase-Glo 3/7 (Promega) according to the manufacturer's instructions. The intensity of luminescence was measured using a FLUOROSCAN instrument (Thermo Scientific). After combination treatment exposure for 7 days (paclitaxel and disulfiram or BAY876) cell viability was quantified using CellTiter-Glo Luminescent Cell Viability Assays (Promega), synergistic interaction was assessed with Combenefit software tool (Di Veroli et al., 2016). All *in vitro* cell-based assays except stem cell frequency assay were performed in quadruplicate and expressed as mean ± SD.

Stem cell frequency assay

Stem cell frequency was calculated with the extreme limiting dilution analysis (ELDA) algorithm (Hu et al., 2009). For *in vitro* analysis, dissociated spheroid cells were seeded into at least 12 wells of the 96-well plate each different cell numbers. After 14 days cultivation, cell clusters > 50 μm in diameter were identified as spheres. To calculate the stem cell frequency after drug exposure, spheroid cells were cultivated with vehicle, paclitaxel, or disulfiram for 7 days. Subsequently, survival dissociated cells were

cultivated in standard cultivation condition for 14 days and counted spheres.

Immunohistochemical analyses

Primary or mouse xenograft tumors were fixed in neutral formalin, embedded in paraffin, and used for staining with hematoxylin and eosin (H&E). For immunostaining, the sections were stained following standard IHC methods, as previously described (Ishiguro et al., 2016), with primary antibodies (Table S4) and biotinylated secondary antibodies (Vector Laboratories, Burlingame, CA, USA), followed by incubation with ABC reagent (Dako) and 3,3'-diaminobenzidine (Sigma).

For staining evaluation, three randomized areas of samples were evaluated by two observers. The extent of staining was visually evaluated on a scale of four levels ("0" indicating no staining to "3" indicating strong staining). Samples with weak, moderate, or strong ALDH1A1 staining (staining intensity scored as 1, 2, or 3, respectively) in at least 10% of cancer cells were regarded as IHC-ALDH-positive, and samples without staining (staining intensity scored as 0) and less than 10% staining of cells were regarded as IHC-ALDH-negative. For evaluating GLUT1 staining, samples with strong staining in at least 50% of cancer cells as IHC-GLUT1-high, and the others were regarded as IHC-GLUT1-low.

Immunocytochemical analyses

Spheroid cells dissociated with Accumax were attached to glass slides using a gelatinizing agent (Smear Gell, Geno Staff), fixed in 4% paraformaldehyde in PBS for 15 min, washed with 1× PBS, permeabilized with PBS/0.1% Triton X-100 for 5 min at 4 °C, and blocked with PBS containing 3% bovine serum albumin. The fixed cells were then used for immunostaining with primary antibodies (Table S4) and secondary Alexa-594 donkey anti-goat antibodies (Abcam), followed by counterstaining with 4',6 diamidino-2-phenylindole.

Quantitative real-time reverse transcription polymerase chain reaction (qRT-PCR) analyses

RNA was isolated from cells with an miRNeasy Micro kit (Qiagen, Valencia, CA, USA), and cDNA was synthesized from total RNA using a PrimeScript First Strand cDNA Synthesis Kit (Takara, Shiga, Japan). Gene expression levels were measured by performing TaqMan gene expression assays (Applied Biosystems/Life Technologies, Carlsbad, CA, USA) with an ALDH1A1 (Hs00946916_m1) or ALDH1A3 (Hs00167476_m1) primer/probe set according to the manufacturer's instructions. Glyceraldehyde 3-phosphate

dehydrogenase was used to calculate delta Ct values for genes.

ECAR measurement

Extracellular acidification rate (ECAR) was measured by the Seahorse XFe-24 Extracellular Flux Analyzer using the Glycolysis Stress Test Kit following the manufacturer's protocol. Cells were seeded at 4×10^5 /well for 24 well plates coated by Poly-D-lysine hydrobromide and centrifuged to attach to the plate. Basal ECAR was measured in glucose-free medium and cells were subjected to sequential injections of glucose 10mM, oligomycin 1.0μM, and 2-deoxyglucose 50mM into the medium.

Metabolic assay

Intracellular Glucose levels and Lactate levels were measured with Glucose-Glo-Assay and Lactate-Glo-Assay (Promega). Glucose uptake of cells was measured with Glucose Uptake-Glo (Promega). All of the measured values were corrected by the number of cells.

Supplemental References

Asano, N., Yoshida, A., Mitani, S., Kobayashi, E., Shiotani, B., Komiyama, M., Fujimoto, H., Chuman, H., Morioka, H., Matsumoto, M., et al. (2017) Frequent amplification of receptor tyrosine kinase genes in welldifferentiated/ dedifferentiated liposarcoma. Oncotarget. 8, 12941-12952.

Di Veroli, G. Y., Fornari, C., Wang, D., Mollard, S., Bramhall, J. L., Richards, F. M. & Jodrell, D. I. (2016) Combenefit: an interactive platform for the analysis and visualization of drug combinations. Bioinformatics. 32, 2866-2868.

Hu, Y. & Smyth, G. K. (2009) ELDA: extreme limiting dilution analysis for comparing depleted and enriched populations in stem cell and other assays. J Immunol Methods. 347, 70-78.

Ishiguro, T., Sato, A., Ohata, H., Ikarashi, Y., Takahashi, R. U., Ochiya, T., Yoshida, M., Tsuda, H., Onda, T., Kato, T., et al. (2016) Establishment and characterization of an in vitro model of ovarian cancer stem-like cells with an enhanced proliferative capacity. Cancer Res. 76, 150-160.

Kato, M., Nakamura, H., Nagai, M., Kubo, T., Elzawahry, A., Totoki, Y., Tanabe, Y., Furukawa, E., Miyamoto, J., Sakamoto, H., et al. (2018) A computational tool to detect DNA alterations tailored to formalin-fixed paraffin-embedded samples in cancer clinical sequencing. Genome Med. 10, 44.

Mootha, V. K., Lindgren, C. M., Eriksson, K. F., Subramanian, A., Sihag, S., Lehar, J., Puigserver, P., Carlsson, E., Ridderstrale, M.,

Laurila, E., et al. (2003) PGC-1alpha-responsive genes involved in oxidative phosphorylation are coordinately downregulated in human diabetes. Nat Genet. 34, 267-273.

Subramanian, A., Tamayo, P., Mootha, V. K., Mukherjee, S., Ebert, B. L., Gillette, M. A., Paulovich, A., Pomeroy, S. L., Golub, T. R., Lander, E. S., et al. (2005) Gene set enrichment analysis: a knowledge-based approach for interpreting genome-wide expression profiles. Proc Natl Acad Sci U S A. 102, 15545-15550.